



# Performance of cement mortar made with recycled high impact polystyrene

Ru Wang<sup>a,b,c,\*</sup>, Christian Meyer<sup>c</sup>

<sup>a</sup> Key Laboratory of Advanced Civil Engineering Materials of Ministry of Education, Tongji University, 4800 Cao'an Road, Shanghai 201804, China

<sup>b</sup> School of Materials Science and Engineering, Tongji University, 4800 Cao'an Road, Shanghai 201804, China

<sup>c</sup> Department of Civil Engineering and Engineering Mechanics, Columbia University, New York, NY 10027, USA

## ARTICLE INFO

### Article history:

Received 7 October 2011

Received in revised form 8 May 2012

Accepted 22 June 2012

Available online 27 June 2012

### Keywords:

Recycled high impact polystyrene (HIPS)

Cement mortar

Strengths

Dynamic modulus of elasticity

Thermal conductivity

Resistance to freeze–thaw cycles

## ABSTRACT

This paper investigates the possibility of utilizing recycled high impact polystyrene (HIPS) as a sand substitute in cement mortar, in order to reduce the solid waste disposal problem and thereby environmental pollution and energy consumption. The results show that the compressive strength and splitting tensile strength of mortar are decreased by replacing sand with HIPS, but the decrease in the splitting tensile strength is much smaller. HIPS makes the mortar become more ductile and increases the energy dissipation capacity. HIPS decreases the dry bulk density, dynamic modulus of elasticity, thermal conductivity, and also water vapor permeability, but does not affect the resistance to freeze–thaw cycles. The use of mortar made with various percentages of HIPS offers promise for applications as medium or light weight concrete, mostly due to its improved thermal isolation, while adding value to a post-consumer plastic material that is now generally treated as solid waste.

© 2012 Elsevier Ltd. All rights reserved.

## 1. Introduction

The unabated growth in the use of plastics in recent years is of considerable concern because of the difficulties involved with their disposal. The reduction of solid waste through reuse or recycling calls for appropriate research efforts. The ideal strategy would be to identify characteristics of value-added applications of recycled plastics. One potential use is as an ingredient of concrete which is the most frequently used construction material in the world because of its known advantageous characteristics. However, its drawbacks are well known, such as low tensile strength and brittleness. In comparison, plastic is more flexible, lighter and tougher, and it has the potential of lower thermal conductivity. If it can be shown that plastic improves certain properties of concrete, it adds value to a material that otherwise would contribute to the solid waste disposal problem.

The idea of using plastic as an ingredient of concrete is not new. Several researchers have studied ways to modify plastic such that it improves certain properties of concrete.

Poly-ethylene terephthalate (PET) aggregates manufactured from waste PET bottles were used as substitute for sand in concrete [1–3]. Such concrete was found to have similar workability characteristics, slightly lower compressive strength and splitting tensile

strength, and moderately higher ductility than the reference concrete. Mortar containing PET and sand aggregate can fall into the structural lightweight concrete category in terms of unit weight and strength properties; i.e. shredded small PET particles may be used successfully as sand substitute in cement composites.

Fibers manufactured from postconsumer plastic milk or water containers were used as substitute for sand in concrete or as reinforcing material [4–6]. Such fibers were shown to arrest the propagation of micro cracks. The inclusion of high density polyethylene (HDPE) fibers did not noticeably improve the splitting tensile strength, but significantly increased the overall toughness, fracture energy, and postpeak load carrying capacity of the cement composite.

River sand was partially replaced by polyvinyl chloride (PVC) waste granules from scrapped PVC pipes [7]. Two major findings were made. On the positive side, the concrete prepared with partial sand replacement by PVC was lighter, more ductile, and had lower drying shrinkage and higher resistance to chloride ion penetration. On the negative side, workability, compressive strength and splitting tensile strength were reduced. In another study [8], ground plastics and glass were used to replace up to 20% of fine aggregates in concrete mixes, while crushed concrete was used to replace up to 20% of coarse aggregates. The investigation revealed that the three types of waste materials can be reused successfully as partial substitutes for sand and coarse aggregate in concrete mixtures.

Some engineering and thermal-setting plastics such as poly(acrylonitrile butadiene styrene)/polycarbonate (ABS/PC), melamine–formaldehyde (MF) and melamine were ground to be used

\* Corresponding author at: Key Laboratory of Advanced Civil Engineering Materials of Ministry of Education, Tongji University, 4800 Cao'an Road, Shanghai 201804, China. Tel.: +86 21 6958 2140.

E-mail address: [ruwang@tongji.edu.cn](mailto:ruwang@tongji.edu.cn) (R. Wang).

in concrete as aggregate substitutes [9–11]. The results showed that with 5% addition of ABS/PC plastic granules the mechanical properties of concrete are increased. Replacing sand with MF resulted in a lighter-weight concrete with improved characteristics, and in general the strengths increased as the percentage of MF was increased, up to a maximum value of approximately 30% MF. The melamine not only led to a low dry density concrete, but also a lower strength.

Recycled HDPE, PVC and polypropylene (PP) were used as coarse aggregates in concrete mixtures to improve the thermal properties of buildings [12]. Some chemical agents were used to treat waste HDPE or ABS powder to be used as additives in concrete with some positive effects [13,14].

Optimal quantities of plastic label waste collected during the glass recycling process were determined for the production of light weight concrete [15]. Some researchers tried to make synthetic lightweight aggregate using recycled PET with granulated blast-furnace slag (GBFS) [16] or HDPE with fly ash [17]. It was found that the adhered GBFS is able to strengthen the surface of waste PET lightweight aggregate and to narrow the transition zone owing to the reaction with calcium hydroxide. The HDPE-fly ash aggregates were manufactured through thermal processing using plastic to encapsulate and bind fly ash particles. As the fly ash content of the aggregates increased, all properties of the concrete were improved.

Recycled PET [18] or mixed plastic and paper waste [19] were processed into fibers to reinforce structural concrete. Both the compressive strength and elastic modulus decreased as fiber volume fraction increased. Cracking due to drying shrinkage was delayed in the PET fiber reinforced concrete specimens. The discrete reinforcement systems derived from abundantly available waste streams can have positive effects on the reinforcement of concrete. If unsaturated polyester based on recycled PET is properly formulated, it can be mixed with inorganic aggregates to produce polymer concrete or polymer mortar with good mechanical properties and durability performance. However, despite the low manufacturing cost of plastic wastes, precast polymer concrete components are not popular in construction because the time-dependent strength development mechanism and mechanical properties are still far from being fully understood [20,21].

High impact polystyrene (HIPS) is a common component of consumer electronics. With the fast increasing use and replacement of such electronics components, the waste disposal problem of HIPS will increase dramatically. This paper investigates the possibility of utilizing recycled HIPS as a sand substitute in cement mortar. If successful, such an application of recycled HIPS will be a major step towards reducing the solid waste disposal problem and reliance on natural resources, thereby reducing environmental pollution and energy consumption.

## 2. Experimental program

### 2.1. Materials and mix design

Type I general-purpose Portland cement according to ASTM C 150/C 150M-09 was used. River sand with a density of 2.44 g/cm<sup>3</sup> and recycled HIPS granules with a density of 1.04 g/cm<sup>3</sup> were used as fine aggregates. The sieve analysis results of the river sand and the ASTM C 33 limits for fine aggregates for concrete are listed in Table 1. The HIPS granules as shown in Fig. 1 were obtained by shredding the HIPS electronics waste to particle size less than 4 mm. Tap water was used in the experiment. The water to cement ratio was 0.55 in all the experiments, the cement to sand ratio is 1:3 for the control, and the mortars with HIPS replacement of sand by volume of 10%, 20% and 50% were also made. The mortar mix designs are listed in Table 2.

**Table 1**  
Sieve analysis results of river sand.

Aperture of sieve (mm)	Passing of river sand (%)	Passing limit in ASTM C 33 (%)
4.75	100.00	95–100
2.36	99.79	80–100
1.18	96.85	50–85
0.84	89.17	–
0.60	79.59	25–60
0.42	62.99	–
0.30	35.78	5–30
0.175	15.66	–
0.150	–	0–10



**Fig. 1.** Picture of HIPS granules.

### 2.2. Production and curing of mortar

The mortar specimens were made and cured according to ASTM C 31/C 31M-09. The cement was mixed with water first, and then the aggregates were added. After mixing, the fresh mortar was filled into cylinder forms with the dimension of  $\phi$  50.8 mm  $\times$  101.6 mm for compressive strength, splitting tensile strength and dry bulk density tests, or  $\phi$  76.2 mm  $\times$  152.4 mm for thermal conductivity, water vapor permeability, dynamic modulus of elasticity and resistance to freezing and thawing tests. The specimens were demolded after 24 h and then cured in 23 °C water until the designed ages.

### 2.3. Test methods

#### 2.3.1. Flow

The flow of the fresh mortar as a measure of workability was determined according to ASTM C 1437-07. The flow value is defined as the average increase in base diameter of the mortar, expressed as a percentage of the original base diameter.

#### 2.3.2. Dry bulk density

The dry bulk density of the mortar was determined according to ASTM C 642-06. The specimens were dried in an oven at a temperature of 105 °C for 72 h before testing. The dry bulk density of the mortar numbers 1, 2, 3 and 4 was 1.98, 1.90, 1.81 and 1.56 g/cm<sup>3</sup>, respectively.

**Table 2**  
Mix designs of mortar.

Number	Cement (g)	Sand (g)	HIPS (g)	Water (g)	Replacement of sand by HIPS (% by volume)
1	100	300	0.0	55	0
2	100	270	12.8	55	10
3	100	240	25.6	55	20
4	100	150	63.9	55	50

### 2.3.3. Compressive strength and dissipated energy

The compressive strength of the mortar was measured according to ASTM C39/C39M-09a, using an Instron 5984 34k Universal Testing Machine. The compressive strength test was stopped when the load decreased by 30% of the maximum value. The dissipated energy per cubic meter was determined as the area under the compressive stress versus strain curve.

### 2.3.4. Splitting tensile strength

The splitting tensile strength of the mortar was determined according to ASTM C 496/C 496M-04, using an Instron 5984 34k Universal Testing Machine. The test was stopped when the load decreased by 30% of the maximum value.

### 2.3.5. Dynamic modulus of elasticity

The dynamic modulus of elasticity of mortar was determined according to ASTM C 215-08. The Olson Instruments Model RT-1 was used to measure the transverse and longitudinal frequencies. The dynamic modulus of elasticity was calculated based on the transverse (or longitudinal) frequency, mass, and dimensions of the test specimen.

### 2.3.6. Thermal conductivity

The radial heat flow method was used to determine the thermal conductivity. This test is designed to simulate a one-dimensional heat flow. Fig. 2 shows the schematic of the test apparatus. Heat is supplied to the system by placing a cartridge heater with a length of 38.2 mm and a diameter of 3.2 mm inside a  $\phi$  76.2 mm  $\times$  76.2 mm concrete cylinder. The temperature is then recorded by placing a thermocouple a short distance away from the heater 19.1 mm below the top of the specimen. The surface of the heater and the thermocouple tip is coated with a highly conductive thermal paste so that their contact resistance between them and the concrete can be neglected.

If the temperature recorded at a point one radius  $r$  away from the heat source is plotted against the natural logarithm of time, the thermal conductivity  $k$  can be determined from the slope of the line (which is denoted as  $m$ ), Eq. (1), where  $Q$  is the power per unit length.

$$K = Q/4\pi m \quad (1)$$

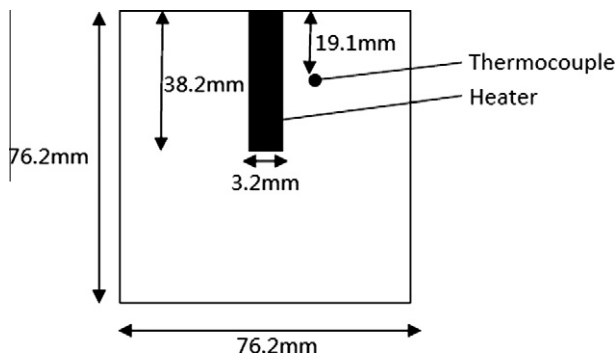


Fig. 2. Schematic apparatus for thermal conductivity test.

If the temperature is recorded at the heater ( $r = 0$ ) then the above approximation is valid for all time values. Since in this experiment the temperature was recorded a short distance away from the heater the approximation cannot be applied to the initial portion of the temperature versus time curve. The test set up is calibrated by testing a material with known thermal conductivity. A piece of corkboard with the same dimensions as the mortar samples was tested and the thermal conductivity was calculated using the above equation. The standard value for thermal conductivity of the corkboard is 0.04 W/m/°C, and the value recorded for the mortar was 0.22 W/m/°C, yielding a calibration coefficient of  $C = 0.18$ . The thermal conductivity can then be expressed as

$$K = CQ/4\pi m \quad (2)$$

It is believed that the coefficient was lower due to the length-to-diameter ratio of the heater and the contact resistance between the heater and inside of the corkboard/concrete. Lobo and Cohen [22] state that if the length to diameter ratio of the heater is less than 20 a portion of the heat does not travel in the assumed radial direction but instead it travels axially. This lowers the effective power of the heater and causes the calibration coefficient to decrease. The length-to-diameter ratio of the heater used in this experiment was 12. Although the calibration coefficient is low in this experiment, the obtained thermal conductivity is comparable.

### 2.3.7. Water vapor permeability

The water vapor permeability of mortar was determined according to ASTM E 96/E 96M-05, using the water method. Test dishes with the dimensions of  $\phi$  70 mm  $\times$  50 mm were used. The water vapor transmission was calculated as follows:

$$Wvt = G/tA = (G/t)/A \quad (3)$$

where  $G$  is the weight change (from the straight line), g;  $t$ , time (h);  $G/t$ , slope of the straight line (g/h);  $A$ , test area (cup mouth area) ( $m^2$ ); and WVT is the rate of water vapor transmission (g/h  $m^2$ ).

The permeance was calculated as follows:

$$Permeance = WVT/\Delta p = WVT/S(R_1 - R_2) \quad (4)$$

where  $\Delta p$  is the vapor pressure difference, mm Hg ( $1.333 \times 10^2$  Pa);  $S$ , the saturation vapor pressure at test temperature, mm Hg ( $1.333 \times 10^2$  Pa), it is 23.76 mm Hg at 25 °C;  $R_1$ , the relative humidity at the source expressed as a fraction (in the dish); and  $R_2$ , the relative humidity at the vapor sink expressed as a fraction.

### 2.3.8. Resistance to freezing and thawing

The resistance to freezing and thawing was determined according to ASTM C666/C666M-03 (Reapproved 2008). The procedure of rapid freezing in air and thawing in water was applied. The freeze-thaw cycle machine manufactured by the Scientemp Company of Adrian, MI, was used. The relative dynamic modulus of elasticity is calculated based on the transverse frequency of a mortar bar according to Eq. (5), and the procedure to measure the transverse frequency is as discussed in Section 2.3.5.

$$P_e = (n_1^2/n^2) \times 100 \quad (5)$$

where  $P_e$  is the relative dynamic modulus of elasticity, after  $c$  cycles of freezing and thawing, percent;  $n$ , the fundamental transverse frequency at 0 cycles of freezing and thawing, and  $n_1$ , the fundamental transverse frequency after  $c$  cycles of freezing and thawing.

The durability factor was calculated as follows:

$$DF = PN/M \quad (6)$$

where  $DF$  is the durability factor of the test specimen;  $P$ , the relative dynamic modulus of elasticity at  $N$  cycles, %;  $N$ , the number of cycles at which  $P$  reaches the specified minimum value for discontinuing the test or the specified number of cycles at which the exposure

is to be terminated, whichever is less, and  $M$  is the specified number of cycles at which the exposure is to be terminated.

### 3. Results and discussion

#### 3.1. Flow

The flow values for mortar numbers 1, 2, 3 and 4 in Table 2 were 90, 97, 92, and 53, respectively. That means HIPS replacement of sand less than 20% does not affect the workability of the mortar significantly, but the flowability becomes bad when the HIPS replacement of sand is 50%. The effect must be result from the HIPS granules' structure that is not so round as the natural sand.

#### 3.2. Compressive strength

The compressive strength of mortar made with various percentages of HIPS at different curing ages is shown in Fig. 3. It indicates clearly that the replacement of sand by HIPS in the mortar reduces the compressive strength almost linearly with the HIPS aggregate replacement ratio. Fig. 4 shows the percentage reduction in compressive strength due to the addition of HIPS aggregates. A reduction in the compressive strength of 12%, 22%, and 49% is obtained, respectively, for mortar with HIPS ratio of 10%, 20%, and 50% at the curing age of 28 days. At curing ages of 3 days and 7 days, the reduction in the compressive strength with 10% and 20% HIPS is not significantly different from that at curing age of 28 days, but with 50% HIPS the reduction in the compressive strength is much less, only about 40%. The reduction in the compressive strength probably comes from the worse connection of the interface between the cement paste and the aggregates, become of the smoother surface of the HIPS granules than natural sand.

Fig. 5 shows the compressive stress versus compressive strain curves of mortar with various percentages of HIPS at different curing ages, with only one curve shown here for one composition. The failure under compression loading of the mortar specimens containing HIPS does not exhibit the typical brittleness normally obtained for regular mortar. The failure observed is more gradual depending on the HIPS content. As the HIPS content increases, the failure type becomes more ductile. The maximum strain increases significantly with the increase of the HIPS ratio (see Table 3). With 10%, 20%, and 50% replacement of sand by HIPS, the maximum strain increases to about 1.1, 1.2, and 1.8 times of that for regular mortar, whatever the curing age. The dissipated energies per cubic meter, i.e. the area under the compressive stress versus compressive strain curves, are also listed in Table 3. The effect of the HIPS on the dissipated energy per cubic meter is not signif-

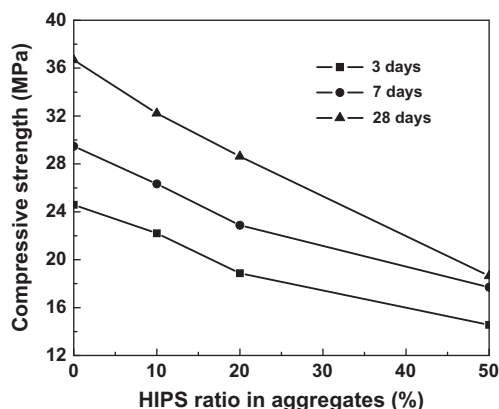


Fig. 3. Compressive strength of mortar at different curing ages.

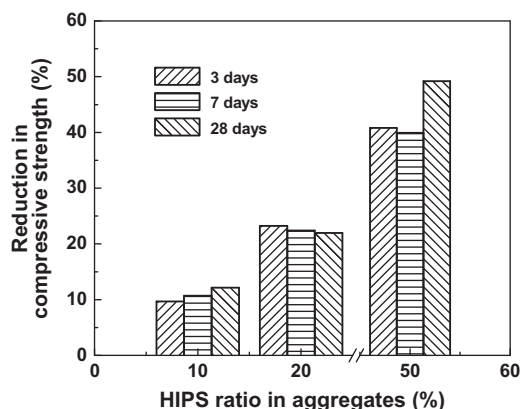


Fig. 4. Reduction in compressive strength of mortar at different curing ages.

icant for replacement ratios up to 20%, but increases markedly if HIPS replaces 50% of the sand.

#### 3.3. Splitting tensile strength

The splitting tensile strength of mortar made with various percentages of HIPS is shown in Figs. 6 and 7 and is found to decrease with increasing HIPS percentage. However, for a HIPS ratio of 10%, the effect on the splitting tensile strength is not significant, especially at curing age of 28 days. The reduction in the splitting tensile strength is more severe as the HIPS percentage increases, but less so at higher curing ages. For the curing age of 28 days, a reduction in the splitting tensile strength of 1.5%, 11%, and 20% was found for mortar made with HIPS of 10%, 20%, and 50%, respectively. It is very clear that the effect of the HIPS on the splitting tensile strength is much smaller than on the compressive strength. That is because although the worse interface between the cement paste and the aggregates affects, the flexible HIPS makes some compensation in splitting tensile strength of the materials.

The ratio of the splitting tensile strength to the compressive strength ( $\sigma_s/\sigma_c$ ) can express to some extent the toughness of cement mortar and is given in Table 4 for various percentages of HIPS. The  $\sigma_s/\sigma_c$  ratio increases by factor 1.12, 1.14, and 1.57 of that of regular mortar with the HIPS ratio of 10%, 20%, and 50%, respectively, at the curing age of 28 days. This is an indication that the toughness of mortar is improved with the replacement of sand by HIPS. That is because that the HIPS is tougher than the natural sand. The curing time also is good for the improvement of the toughness.

#### 3.4. Dynamic modulus of elasticity

The dynamic modulus of elasticity of mortar made with various percentages of HIPS is listed in Table 5. It decreases as the percentage of HIPS increases. This fact is related to the reduction in the bulk density of the mortar and can be attributed to the low modulus of the HIPS. This softening of the cement mortar is already illustrated by the compressive stress versus compressive strain curves as discussed in Section 3.1.

#### 3.5. Thermal conductivity

Six to eight specimens for each mortar composition were tested to determine the thermal conductivity. The temperature versus natural logarithm of time curves of mortar made with various percentages of HIPS are shown in Fig. 8. The corresponding thermal conductivities are shown in Table 6. It is noteworthy that the HIPS



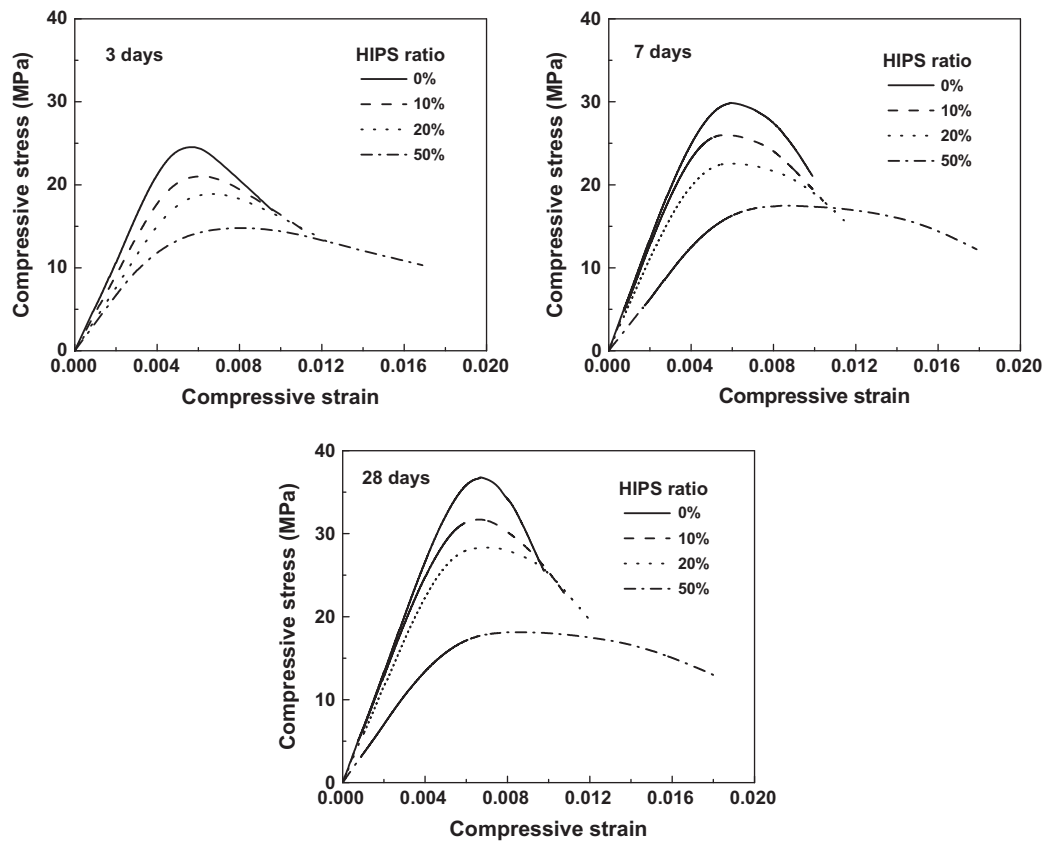


Fig. 5. Compressive stress versus compressive strain curves of mortar at different curing ages.

Table 3

Maximum strain and dissipation energy of mortar during the compressive strength test.

HIPS ratio in aggregates (%)	Maximum strain				Dissipated energy (kJ/m <sup>3</sup> )			
	0	10	20	50	0	10	20	50
3 days	0.0095	0.0109	0.0116	0.0174	169	176	160	199
7 days	0.0100	0.0109	0.0120	0.0165	214	212	210	234
28 days	0.0096	0.0109	0.0114	0.0175	240	242	239	256

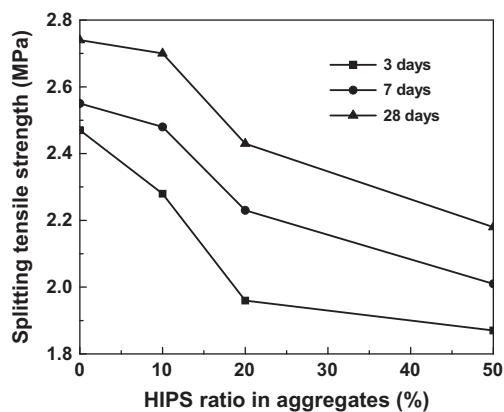


Fig. 6. Splitting tensile strength of mortar at different curing ages.

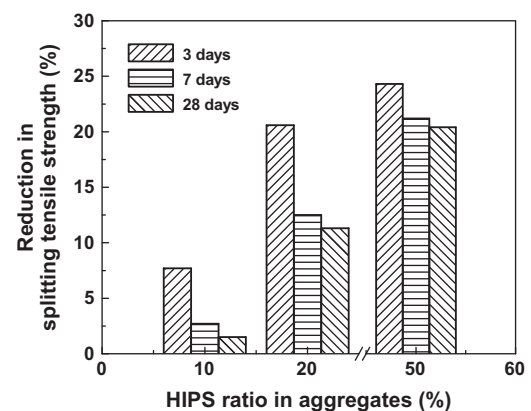


Fig. 7. Reduction in splitting tensile strength of mortar at different curing ages.

decreases the thermal conductivity of mortar, namely to 87%, 69% and 44% of that of regular mortar with 10%, 20% and 50% HIPS replacement of sand, respectively. This is due to the low thermal conductivity of the HIPS compared with that of natural sand and the lower bulk density of mortar made with HIPS.

### 3.6. Water vapor permeability

The water vapor permeability and permeance of mortar made with various percentages of HIPS calculated according to Eqs. (3) and (4) are listed in Table 7. The replacement of sand by HIPS

**Table 4**

Ratio of splitting tensile strength to compressive strength of mortar.

Curing ages (day)	3	7	28
HIPS replacement ratio of sand (%)			
0	0.100	0.086	0.075
10	0.103	0.094	0.084
20	0.104	0.097	0.085
50	0.129	0.113	0.117

**Table 5**

Dynamic modulus of elasticity of mortar.

HIPS ratio in aggregates (%)	0	10	20	50
Dynamic modulus of elasticity (GPa)	36	30	25	13

decreases the water vapor permeability of mortar from 1.45 g/(h m<sup>2</sup>) to 1.25 g/(h m<sup>2</sup>) as the HIPS content increases from 0 to 50%. The permeance decreases slightly with the increase of HIPS content. That is probably because of the larger hydrophobicity of plastics compared with the natural sand. It is clear that the effect of the HIPS on the water vapor permeability of mortar is not significant and the recorded values are acceptable for most applications.

### 3.7. Resistance to freezing and thawing

The durability of concrete is of considerable importance for most applications. Although many durability characteristics correlate strongly with mechanical strength, very often, separate tests need to be performed to directly determine the durability in order

to ascertain whether the concrete structure or product will maintain its properties throughout its intended service life. The degradation caused by cycles of freezing and thawing is particularly important in Northern climates. The relative dynamic moduli of mortar made with different percentages of HIPS after various freeze–thaw cycles are listed in Table 8. It is interesting to find that the relative dynamic modulus remains constant up to 300 freeze–thaw cycles for all mortars, regardless of the HIPS replacement ratio. Thus, according to ASTM the mortar passes the freeze–thaw cycle test, and the use of HIPS as partial replacement of sand does not affect the mortar's resistance to freezing and thawing.

## 4. Summary

The following conclusions can be drawn from the study reported herein:

- The compressive strength and splitting tensile strength of mortar are decreased by replacing sand with HIPS, but the decrease in the splitting tensile strength is much smaller than that of the compressive strength. A reduction in the compressive strength of 12%, 22%, and 49% is obtained for mortar containing 10%, 20%, and 50% HIPS, respectively. However, a reduction in the splitting tensile strength of 1.5%, 11%, and 20% is obtained for mortar containing 10%, 20%, and 50% HIPS, respectively.
- As HIPS content increases, the failure type of the mortar becomes more ductile, and the maximum strain increases significantly to 1.1, 1.2, and 1.8 times of that for regular mortar when the HIPS ratio is 10%, 20%, and 50%, respectively. At the same time, HIPS increases the dissipated energy per cubic meter of mortar.

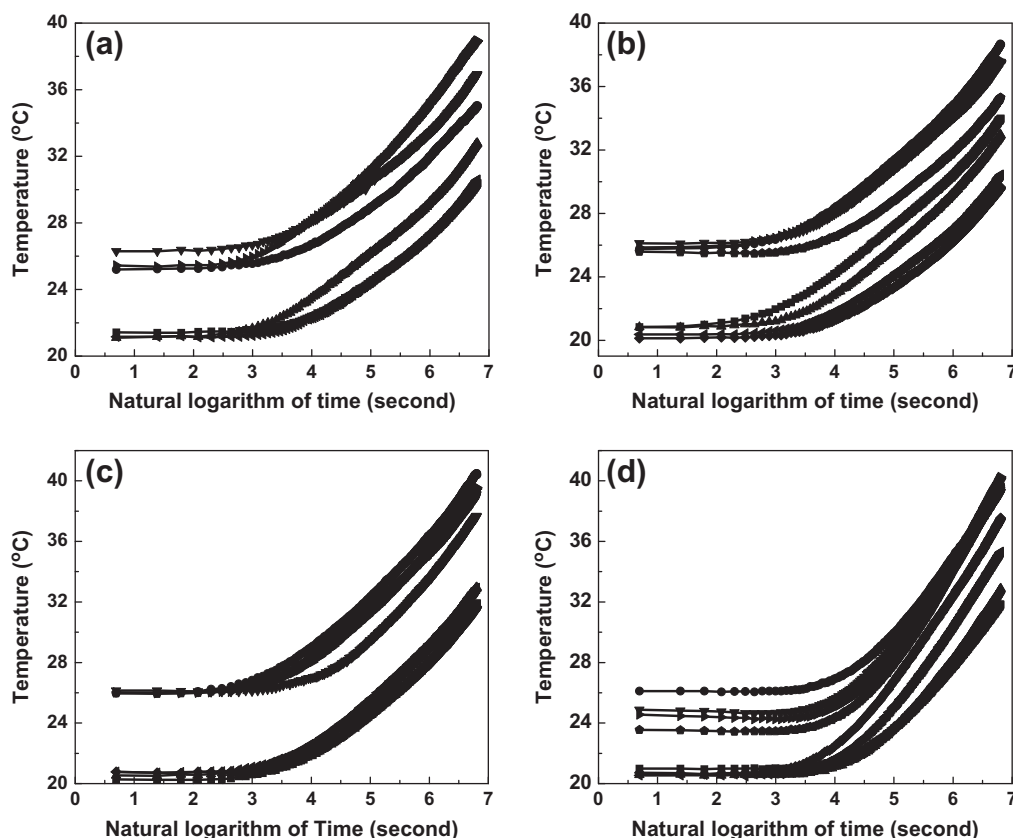


**Fig. 8.** Temperature versus natural logarithm of time for mortar made with (a) 0, (b) 10%, (c) 20%, and (d) 50% HIPS replacement of sand.

**Table 6**

Thermal conductivity of mortar.

HIPS ratio in aggregates (%)	0	10	20	50
Thermal conductivity (W/m/°C)	0.61	0.53	0.42	0.27

**Table 7**

Water vapor permeability and permeance of mortar.

HIPS ratio in aggregates (%)	0	10	20	50
Water vapor permeability (g/(h m <sup>2</sup> ))	1.45	1.44	1.32	1.25
Permeance (g/(h m <sup>2</sup> mm Hg))	0.08	0.08	0.07	0.07

**Table 8**

Relative dynamic modulus of elasticity of mortar.

Cycles	HIPS ratio in aggregates (%)			
	0	10	20	50
17	101	100	102	102
40	101	99	103	101
57	101	100	102	102
79	101	100	102	101
97	101	100	102	101
121	101	100	102	100
139	102	101	102	100
162	102	102	104	103
179	102	103	103	103
203	103	103	103	102
220	102	103	104	103
244	102	103	104	101
261	102	103	104	102
285	102	103	103	102
300	103	103	104	102

- The dynamic modulus of elasticity of mortar is found to decrease from 36 GPa to 30 GPa, 25 GPa, and 13 GPa when increasing the HIPS ratio from 0 to 10%, 20%, and 50%, respectively.
- HIPS decreases the dry bulk density of mortar. With 10% and 20% HIPS replacement, the mortar qualified as medium weight concrete, and with 50% HIPS, it qualified as light weight concrete.
- The thermal conductivity of the mortar decreases to 87%, 69%, and 44% that of regular mortar when the HIPS ratio is 10%, 20%, and 50%, respectively.
- HIPS decreases the mortar's water vapor permeability, and it does not affect the freeze–thaw cycle resistance.
- The use of mortar made with various percentages of HIPS offers promise for applications as medium or light weight concrete, mostly due to its improved thermal insulation, while adding value to a post-consumer plastic material that is now generally treated as solid waste.

## Acknowledgments

The research reported herein was financially supported by the China Scholarship Council and the Fundamental Research Funds for the Central Universities (Tongji University: 0500219146). The authors are grateful for helpful support received from the Lab Manager Adrian Brügger, the Associate Research Scientist Liming Li of the Carleton Laboratory, and the PhD students Xueyu Pang and Dan Hochstein. Support by Columbia University and Carleton Laboratory is also gratefully acknowledged.

## References

- [1] Frigione M. Recycling of PET bottles as fine aggregate in concrete. *Waste Manage* 2010;30:1101–6.
- [2] Akcaozoglu S, Atis CD, Akcaozoglu K. An investigation on the use of shredded waste PET bottles as aggregate in lightweight concrete. *Waste Manage* 2010;30:285–90.
- [3] Marzouk OY, Dheilily RM, Queneudec M. Valorization of post-consumer waste plastic in cementitious concrete composites. *Waste Manage* 2007;27:310–8.
- [4] Ismail ZZ, AL-Hashmi EA. Use of waste plastic in concrete mixture as aggregate replacement. *Waste Manage* 2008;28:2041–7.
- [5] Sobhan K, Mashnad M. Tensile strength and toughness of soil–cement–fly-ash composite reinforced with recycled high-density polyethylene strips. *J Mater Civ Eng* 2002;14(2):177–84.
- [6] Sobhan K, Mashnad M. Mechanical stabilization of cemented soil–fly ash mixtures with recycled plastic strips. *J Environ Eng* 2003;129(10):943–7.
- [7] Kou SC, Lee G, Poon CS, Lai WL. Properties of lightweight aggregate concrete prepared with PVC granules derived from scraped PVC pipes. *Waste Manage* 2009;29:621–8.
- [8] Batayneh M, Marie I, Asi I. Use of selected waste materials in concrete mixes. *Waste Manage* 2007;27:1870–6.
- [9] Li LJ, Huang HB, Liu F. Experimental study on mechanical properties of concrete with recycled plastic granules. *Build Mater Green Build* 2009;263–6.
- [10] Dweik HS, Ziara MM, Hadidoun MS. Enhancing concrete strength and thermal insulation using thermoset plastic waste. *Int J Polym Mater* 2008;57(7):635–56.
- [11] Phaiboon P, Mallika P. Reuse of thermosetting plastic waste for lightweight concrete. *Waste Manage* 2008;28(9):1581–8.
- [12] Elzafraney M, Soroushian P, Deru M. Development of energy-efficient concrete buildings using recycled plastic aggregates. *J Archit Eng* 2005;11(4):122–30.
- [13] Naik TR, Singh SS, Huber CO, Brodersen BS. Use of post-consumer waste plastics in cement-based composites. *Cem Concr Res* 1996;26(10):1489–92.
- [14] Palos A, Souza NAD, Snively CT, Reidy RF. Modification of cement mortar with recycled ABS. *Cem Concr Res* 2001;31:1003–7.
- [15] Koonthong S, Chawakitchareon P, Chalee W. Optimize quantities of plastic label waste for making light weight concrete. In: 35th congress on science and technology of Thailand; 2009. p. 1–5.
- [16] Choi YW, Moon DJ, Chung JS, Cho SK. Effects of waste PET bottles aggregate on the properties of concrete. *Cem Concr Res* 2005;35:776–81.
- [17] Jansen DC, Kiggins ML, Swan CW, Malloy RA, Kashi MG, Chan RA. Lightweight fly ash-plastic aggregates in concrete. *J Trans Res Board* 2001;1775:44–52.
- [18] Kim SB, Yi NH, Kim HY, Kim JH, Song YC. Material and structural performance evaluation of recycled PET fiber reinforced concrete. *Cem Concr Compos* 2010;32:232–40.
- [19] Soroushian P, Plasencia J, Ravanbakhsh S. Assessment of reinforcing effects of recycled plastic and paper in concrete. *ACI Mater J* 2003;100(3):203–7.
- [20] Rebeiz KS, Fowler DW, Paul DR. Polymer concrete and polymer mortar using resins based on recycled poly (ethylene terephthalate). *J Appl Polym Sci* 1992;44:1649–55.
- [21] Jo BW, Park SK, Kim CH. Mechanical properties of polyester polymer concrete using recycled polyethylene terephthalate. *ACI Struct J* 2006;103(2):219–25.
- [22] Lobo H, Cohen C. Measurement of thermal conductivity of polymer melts by the line-source method. *Polym Eng Sci* 1990;30(2):65–70.